Journal of Molecular Liquids 365 (2022) 120209

Contents lists available at ScienceDirect

Journal of Molecular Liquids

journal homepage: www.elsevier.com/locate/molliq

Trifluoroethanol direct interactions with protein backbones destabilize α-helices

Ander F. Pereira [1], Vinicius Piccoli [1], Leandro Martínez *

Institute of Chemistry and Center for Computing in Engineering & Science, University of Campinas, Campinas, SP, Brazil

ARTICLE INFO

Article history:
Received 27 April 2022
Revised 18 July 2022
Accepted 23 August 2022
Available online 28 August 2022

Keywords:
2,2,2-Trifluoroethanol
Helices
Solvation
Protein folding

ABSTRACT

2,2,2-Trifluoroethanol (TFE) is a well-known protein α-helix stabilizer; nevertheless, after much investigation, no consensus has been reached on TFE's stabilizing mechanism. TFE alters the structure of water and affects its dielectric properties, but also competes with it for hydrogen bonds with the backbone and side chains of proteins. Thus, indirect and direct mechanisms of TFE activity have been proposed. The direct mode is especially appealing: TFE establishes hydrogen bonds with the carbonyls of the peptides' backbones, eliminating water, apparently protecting the intra-helix hydrogen bond. Because these interactions occur simultaneously with other changes in the solution structure, it is difficult to disentangle the contribution of direct vs. indirect processes to the TFE stabilizing effect. Here, we perform extensive enhanced sampling simulations of the $(AAQAA)_3$ peptide in mixtures of water and TFE at various concentrations. Minimum-distance distribution functions (MDDFs) and the Kirkwood-Buff (KB) theory of solutions are used to understand the molecular and thermodynamic basis of the TFE mechanism of α-helix stabilization. The simulations confirm the stabilizing role of TFE on the helical content of the peptide and that the helical structures are preferentially solvated by TFE. TFE effectively interacts with the protein backbone, excluding water, in agreement with the direct-interaction model. Yet, simulations allow alchemical experiments to be performed, and thus we modified the intermolecular backbone-TFE interactions to prevent the putatively stabilizing hydrogen-bond. Surprisingly, the peptide's helical content increased, showing that these direct contacts have a denaturing effective contribution. At the same time, the preferential interaction parameters remain basically constant in the absence of the TFE-backbone hydrogen bonds. Therefore, the model of TFE helix stabilization based on the protection of backbone hydrogen bonds by hydrogen-bonding the backbone's carbonyl is not supported by evidence. We show that TFE non-specific interactions with the helical conformations are stronger than with the coil states, excluding water.

1. Introduction

The fluorinated alcohol 2,2,2-Trifluoroethanol (TFE) is a well-known stabilizer of the α-helical structures of peptides and proteins. The mechanisms for this stabilization are thoroughly investigated [1,2]. TFE effects on protein structures can be rationalized in terms of many physical phenomena, because as a cosolvent it perturbs the structure of water [2–4], lowers dramatically the dielectric constant of the solution [5], forms clusters [6,7], promotes preferential hydrophobic solvation [8,9], and, additionally, is able to form hydrogen bonds with the protein, with the backbone in particular [1,2]. Because of this plethora of effects on the solution structure and interactions, the stabilizing role of TFE on helices is difficult to rationalize. For instance, various experimental studies demonstrate that TFE interacts directly with the protein structure excluding water molecules [5,10,11], interactions that are confirmed by molecular dynamics (MD) simulations [3,11]. According to these findings, TFE also lowers the frequency of persistent protein-water hydrogen bonds, particularly with the backbone atoms.

TFE is able to form a hydrogen bond with the backbone carbonyl atom, as shown in Fig. 1 [1,2]. This interaction apparently does not interfere with the helix's intramolecular hydrogen bond and prevents water from doing so [1,2]. From this observation, a structurally appealing direct-interaction mechanism for helix stabilization can be proposed. However, equilibrium hydrogen isotope partitioning measurements, indicated that intra-helical

* Corresponding author at: Institute of Chemistry, University of Campinas, 13083-970 Campinas, SP, Brazil.
E-mail address: lmartine@unicamp.br (L. Martínez).
[1] These authors contributed equally to this work.

https://doi.org/10.1016/j.molliq.2022.120209
0167-7322/

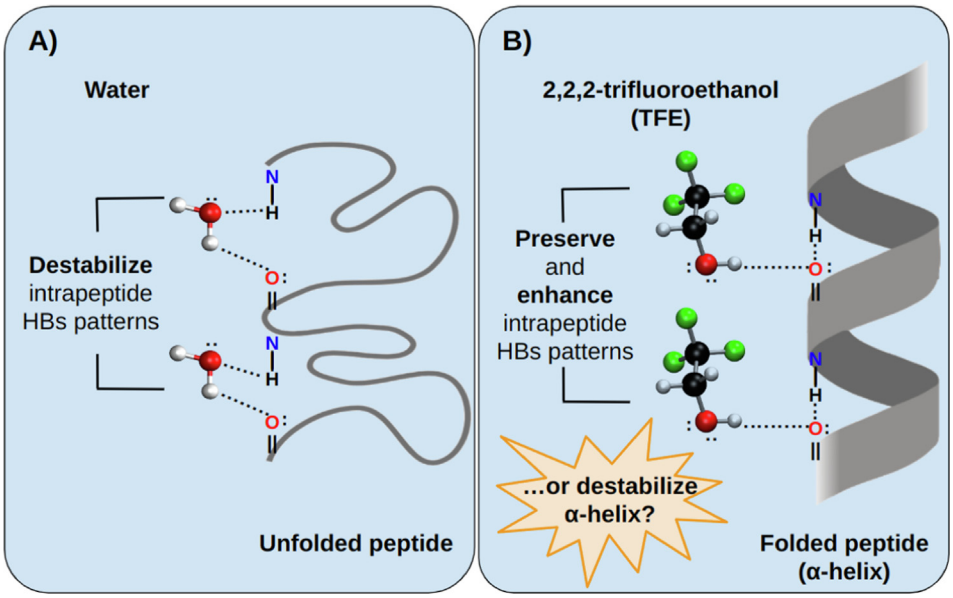

Fig. 1. Hydrogen bonding models of A) water and B) TFE with the helix backbone. Water molecules act as both H-bond donors and acceptors, causing the peptide's intramolecular H-bonds to be disrupted. On the other hand, TFE is a strong H-bond donor but a poor acceptor [5]. As a result, it was proposed that the acidic hydrogen of TFE can interact with the oxygen of the backbone while protecting the peptide's intramolecular H-bonds (N-H···O) that stabilize the helix [1,2]. Figure adapted from reference [1].

hydrogen-bonds are not strengthened by the presence of TFE [12], suggesting that the stabilization occurs by reinforcing the structure of the solution, which increases the energetic cost of the solvation of the unfolded peptide surface. Thus, the mechanism of TFE helix stabilization was rationalized also in terms of the preferential interaction of the helical structures or by the indirect perturbation of the water structure [3,11,13,14]. It is of course possible that both direct and indirect mechanisms cooperate to stabilize the helices. Probing the contribution of each mechanism to the overall stabilization effect is difficult, particularly with experimental approaches.

In this work, we conduct extensive enhanced-sampling molecular dynamics simulations of the conformational equilibrium of the Ace-AAQAAAAQAAAAQAA-NH_2 ($AAQAA_3$) peptide in water and in various concentrations of TFE. This peptide displays a model helical structure in water, and is used in experimental and computational investigations of the role of cosolvents on helix stability [15–21]. By analyzing the solution structure and thermodynamics using Minimum-Distance Distribution Functions and the Kirkwood-Buff theory of solvation, we are able to describe the accumulation of TFE on the surface of the peptide and its effect on the hydrogen bond network of the solution. We confirm the current structural and thermodynamic pictures of TFE's interactions with the peptide matrix. However, in what follows, we modify the TFE-backbone interaction potential to impair the formation of hydrogen bonds, and show that this leads, perhaps unexpectedly, to the potentialization of the TFE helix stabilizing effect. This implies that despite the direct backbone-TFE interactions, the helical structure is maintained via mechanisms linked to the structure of the solution and/or to the exclusion of water from the protein neighborhood by non-specific preferential solvation.

2. Methods

2.1. Molecular dynamics simulations

Various algorithms have been used to improve the sampling in molecular dynamics, such as replica-exchange molecular dynamics (REMD) [22–24], metadynamics [25], and simulated annealing [25,26]. The method Temperature Replica Exchange Method (TREM) in particular has garnered recognition for being conceptually sound and practical, particularly for being trivially parallelizable [27–29]. Regrettably, the number of replicas required to obtain a representative sample increases linearly with the square root of the total number of degrees of freedom in the system [30]. To address this issue, a variant of this technology called Replica Exchange with Solute Tempering (REST1) was developed [31,32]. REST1 effectively heats only the solute while leaving the solvent unchanged. REST1 is more efficient than TREM when applied to tiny solutes such as the alanine dipeptide; but, when applied to large systems, REST1 can be even less efficient than TREM [31,32].

To compensate for REST1's inefficient sampling, the method Replica Exchange with Solute Tempering-2 (REST2) was developed [30]. REST2 was found to sample the conformation space more efficiently than REST1 [30]. The modified scaling of the Hamiltonian is employed in the REST2 algorithm to alter the parameters of the force fields, allowing the entire system to be heated [33,34]. In this work, we employed the REST2 method [30] to study the effect of TFE in the conformational stability of the $AAQAA_3$. By using this accelerated sampling strategy and modern computer facilities, we are able to probe a converged equilibrium ensemble of the folding reaction and to compute the solvent structure and thermodynamics in detail. Some of our results corroborate previous qualitative simulation studies of TFE mechanisms of helix protection [3], within a rigorous thermodynamic framework.

All simulations were performed in the software GROMACS (v2019.4) [35] patched with PLUMED (v2.5.5) [36] at the temperature of 300 K. In REST2, all replicas are run at the same temperature, but the potential energy for each replica m is scaled according to Eq. (1):

$$E_m^{REST}(X) = \frac{\beta_m}{\beta_0}E_{pp}(X) + \sqrt{\frac{\beta_m}{\beta_0}E_{ps}(X)} + E_{ss}(X) \quad (1)$$

where E_{pp} is the peptide intramolecular energy, E_{ps} is the peptide-solvent interaction energy and E_{ss} is solvent–solvent interaction energy; X represents the configuration of the whole system; $\beta_m = 1/k_B T_m$ and T_0 is the temperature of interest. Here, 10 replicas

were adopted for each system, and E_{pp} and E_{ps} were scaled by a β_m/β_0 and $\sqrt{(\beta_m/\beta_0)}$, respectively, with β_m/β_0 varying from 1 to 0.5245. Each system was initially minimized by 1000 steepest descent steps, followed by two 1 ns simulations of equilibration at NVT and NPT ensembles. Following the equilibration steps, each replica was simulated on the NPT ensemble for 500 ns (totalling 5 μs for each system, considering the replicas), with exchange attempts every 400 MD steps. The range of perturbations was set such that an acceptance ratio above 30 % was obtained. Structures were saved every 500 ps. Simulations were performed at a constant pressure of 1 bar using the Parrinello-Rahman [37] algorithm with a relaxation time of 2 ps and isothermal compressibility of 4.5×10^{-5} bar^{-1}. A stochastic velocity-rescaling thermostat was used to control the temperature with a 0.1 ps period [38]. Periodic boundary conditions were applied, and a cutoff of 1.2 nm was used for short-range interactions. Long-range electrostatic interactions were calculated by Particle-Mesh Ewald (PME) [39] summation method with a fourth-order interpolation and a grid spacing of 0.16 nm. All bonds involving hydrogen atoms were constrained with the LINCS algorithm [40]. To integrate the equations of motion, the leap-frog algorithm was used with a time step of 2 fs. For analyses, only the replica 0 was used.

An initial configuration of $AAQAA_3$ was built with the Visual Molecular Dynamics (VMD) package [41]. Then, $AAQAA_3$ was solvated in cubic boxes of 56 Å with Packmol [42,43], containing different concentrations of the water and TFE according to Table 1. All systems were simulated with the TIP4P/2005 water model [44], and the amber03w force field [45] for the peptide. Cosolvent molecules (TFE) were simulated with a model previously developed to reproduce thermodynamic properties of pure TFE and water-TFE mixtures [46]. The same set of parameters was used and validated in previous works to understand the effect of TFE on helix stability [9]. The simulations slightly underestimated the helical content of the peptide in water (see Fig. 2), as judged by the results of Shalango et al. [20], and this is a known limitation of the force-field for proteins in the presence of the current water model [47]. Nevertheless, the compatibility of the force fields of water and cosolvent was preferred [9].

Finally, we performed similar simulations of the peptide in TFE solutions, in which the intermolecular hydrogen bonds between the hydroxyl oxygen of TFE and the oxygen of the backbone were inhibited by increasing the Van-der-Waals exclusion radius associated with these atom pairs only. Specifically, σ_{ij} was multiplicated by a scaling factor γ of 1.5 within the Lorentz-Berthelot combination rule ($\sigma_{ij} = \gamma((\sigma_i + \sigma_j)/2)$, where σ_i is the hydroxyl oxygen parameter of TFE (atom type oh) and σ_j is the parameter of the peptide's carbonyl oxygen atom (atom type O). These atoms were chosen because σ is zero for the hydrogen atom of TFE in the force-field.

From the simulations with the modified potential, we explore the role of TFE-backbone hydrogen bonds in the stability of the helix with similar protocols as the ones described above. In total, 13 systems were simulated, summing up 65 μs of simulations. The convergence of the simulations was accessed by computing standard errors of the estimates and the auto-correlation functions of the average peptide helical content in all simulations (Supplementary Material - Section 2). The helical content was uncorrelated after ~50 ns in the simulations, and the averages computed from blocks do not deviate from the estimates from full sampling enough to invalidate the stabilizing effect of TFE. Since the REST2 simulations were performed for 500 ns, we believe that the results are reasonably well converged for the purposes of the current analyses.

2.2. Calculation of peptide ellipticity

The secondary structure assignment for each peptide residue in the simulations was performed with the DSSP software (version 3.0.0) [48]. Theoretical Circular Dichroism (CD) spectra of the $AAQAA_3$ peptide in water were calculated with SESCA [49] and compared with experimental results obtained from Ref. [20]. Theoretical spectra were calculated with recommended basis sets for three algorithms (DSSP [48], DISICL [50], and HbSS [49]), which evaluate the contribution of the backbone (DSSP-T, DISICL-dT, and HBSS-3 basis set) and side chains (DSSP-1SC3, DISICL-dTSC3, and HBSS-3SC1 bases set) in predicting the CD spectra. After evaluating the agreement between theoretical and experimental spectra of the peptide in water, we adopted the HBSS-3SC1 basis set for all calculations.

Table 1
Compositions of the molecular systems simulated with different concentrations of 2,2,2-Trifluorethanol (TFE).

Systems	Number of water molecules	Number of TFE molecules
$AAQAA_3$ – 0 % v/v	5805	0
$AAQAA_3$ – 20 % v/v	4703	289
$AAQAA_3$ – 40 % v/v	3584	578
$AAQAA_3$ – 50 % v/v	3003	723
$AAQAA_3$ – 60 % v/v	2417	868
$AAQAA_3$ – 80 % v/v	1214	1158
$AAQAA_3$ – 100 % v/v	0	1448

2.3. Minimum-distance distribution functions and solvation thermodynamics

In this section we provide an overview of the formalism and computational methods to obtain distribution functions, Kirkwood-Buff integrals, and preferential interaction parameters, which were computed with the ComplexMixtures.jl package [51]. More detailed accounts of the theory are provided in previous publications [52–54]. In this work, we study tertiary solutions containing a peptide (species p), water (species w), and the TFE cosolute (species c). The peptide will be considered at infinite dilution and the molar concentrations of water and cosolvent are, respectively, ρ_w and ρ_c. The cosolvent distribution around the peptide in the solution can be described in terms of the average number density of cosolvents $n_c(r)$ relative to the density of an ideal-gas distribution, $n_c^*(r)$,

$$g_{pc}(r) = \frac{n_c(r)}{n_c^*(r)} \tag{2}$$

where r is the distance between the peptide and the cosolvent. Here, we use the minimum distance between any atom of the peptide and any atom of the solvent, which defines the minimum-distance distribution function (MDDF). The use of MDDFs is important in the present study as they adapt to the shape of the solute and the solvent, and can then be used to to provide a molecular picture of the solvation of the helical and coil conformations of the peptide. Also, MDDFs can be used to compute Kirkwood-Buff integrals and preferential interaction parameters [55,56], connecting the microscopic view of solvation with thermodynamic parameters.

The Kirkwood-buff integrals can be calculated using $n_c(r)$ and $n_c^*(r)$,

$$G_{pc} = \frac{1}{\rho_c}\int_0^\infty [n_c(r) - n_c^*(r)]S(r)dr \tag{3}$$

where $S(r)$ is the surface defined by the minimum-distance r to any atom of the solute. Due to the minimum-distance count, $S(r)$ is dependent on the solute's shape. By the integration of Eq. (2), we obtain, for a finite sub-volume of the system,

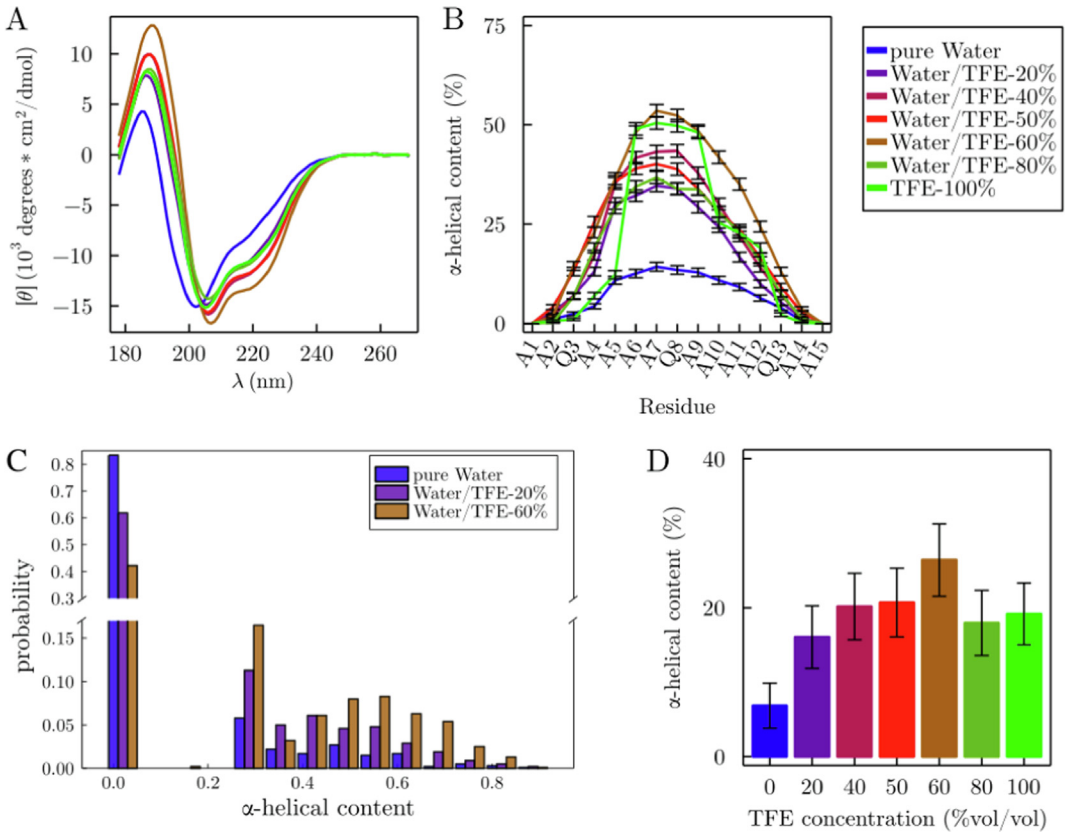

Fig. 2. Structural properties of the $AAQAA_3$ peptide in water (blue) and aqueous solutions of TFE, computed from the simulations: A) Circular dichroism (CD) spectra. TFE increases the helical content of the peptide, as shown by the increased band at ~190 nm and by the characteristic double-dip at 200–230 nm. B) Average per-residue α-helix prevalence. C) Probability density of the peptide helical content (supplementary Figure S5 displays the data for all concentrations). D) Average ellipticity of the peptide in each solution. Error bars in the figures indicate the standard deviations of the mean of the quantities computed. (For interpretation of the references to colour in this figure legend, the reader is referred to the web version of this article.)

$$G_{pc}(R) = \frac{1}{\rho_c}\left[N_{pc}(R) - N^*_{pc}(R)\right] \tag{4}$$

Where $N_{pc}(R)$ and $N^*_{pc}(R)$ are, respectively, the number of minimum-distances between the protein and the solvent smaller than R, and the number of equivalent distances within R in a system with ideal-gas distribution (i e. in the absence of solute–solvent interactions) [52–54].

The protein domain is the region of the solution around the protein where protein-solvent interactions cannot be considered negligible. The Kirkwood-Buff integrals represented by the Eqs. (3) and (4) are the excess volume occupied by the cosolvent in the protein domain, relative to the volume that the cosolvent would occupy if there were no solute–solvent interactions [57–59]. Favorable protein-solvent interactions will be indicated by positive KB integrals value. On the other hand, if the protein-solvent interactions are unfavorable, the solvent's concentration in the protein domain will be smaller in comparison to bulk, resulting in a negative KB integral.

The preferential solvation parameter is a thermodynamic quantity that can be experimentally measured by techniques like equilibrium dialysis and vapor pressure osmometry [60,61]. It provides a quantification of the interaction of cosolvent with biomolecules, and it can be defined as.

$$\Gamma = \left(\frac{\partial \mu_p}{\partial \mu_c}\right)_{m_p,T,P} = \left(\frac{\partial m_c}{\partial m_p}\right)_{\mu_c,T,P} \tag{5}$$

where μ is the chemical potential and m is the concentration. Its meaning is the change of the protein chemical potential of a solute in response to the variation of the concentration of a cosolvent in the solution [62,63].

The preferential solvation parameter can be computed from the difference of KB integrals of the solvent components and gives the information of which component is preferentially bound to the solute [57,64,65]. In the context of this work, where we are working with ternary solutions and the solute (the protein) is considered infinitely diluted, the cosolvent TFE preferential binding to the protein, relative to water is.

$$\Gamma_{pc}(R) \approx \rho_c\left[G_{pc}(R) - G_{pw}(R)\right] \tag{6}$$

and consists of the number of cosolvent molecules in excess or deficit in the protein domain, considering the cosolvent molecular volume in the bulk solution. The binding of water relative to the cosolvent can be provided by the preferential hydration parameter.

$$\Gamma_{pw}(R) \approx \rho_w\left[G_{pw}(R) - G_{pc}(R)\right] \tag{7}$$

A positive value for $\Gamma_{pc}(R)$ and a negative value for $\Gamma_{pw}(R)$ mean that the cosolvent accumulates in the protein domain - the protein is effectively dehydrated.

The MDDFs were calculated using a discretized version of Eq (2) in which the density was computed from the average number of minimum-distances at each 0.1 Å bin. The KB integrals and preferential interaction parameters for the cosolvent were computed according to Eqs. (4) and (6), and the preferential hydration parameter according to Eq (7). We used R = 15 Å, which is larger than typically used for computing KB integrals in protein-solvent systems [66]. With that cutoff, we obtained reasonably well converged integrals in most simulations, and preferential solvation parameters were clear.

3. Results and discussion

3.1. TFE stabilizes $AAQAA_3$ helical structure

In Fig. 2 we provide an overview of the structural properties of the $AAQAA_3$ as obtained from the enhanced sampling molecular dynamics simulations. Fig. 2A displays the computed circular-dichroism (CD) spectra of the peptide in water (blue) and aqueous TFE solutions. It is evident that the α-helix content of the peptide is always higher in the presence of TFE than in pure water. In the spectrum of the peptide in the water, there is a positive band at 184 nm and a negative band at 202 nm, in agreement with the experimental observation [20]. The second negative band around 220 nm, characteristic of α-helices, is not well defined, but as the concentration of TFE increases in the solution, it is possible to observe the build up of the dip in 221 nm.

As shown in Fig. 2B, the per-residue α-helix content of the peptide in TFE is considerably higher than in pure water, even in the lowest concentrations of the cosolvent. The helical propensity of the residues of the center of the peptide is the greater. In pure TFE the central residues retain their helical behavior, but residues closer to the terminal groups lose their ellipticity. It is important to remark that in all simulations fluctuations occurred such that the peptide visited conformations with high and low helical contents (Fig. 2C and Supplementary Figure S5). Yet, the population of the coiled state in water is maximal, and it is minimal in the 60 % vol/vol TFE solution.

The maximum ellipticity of the peptide is observed at 60 %-TFE, as shown in Fig. 2D. This is in agreement with the fact that the helical content of alanine-rich peptides [67–69], and also of peptides and proteins of distinct sequences [70–73], are maximal in aqueous solutions of TFE, and not in the pure cosolvent. The rationale for the presence of this maximum in helical stability as a function of concentration is not well understood [74], particularly for being dependent on the amino acid sequence [5,68]. Some authors suggest that the decrease in ellipticity with increasing concentration of TFE is related to the disruption of hydrophobic components of the interactions that maintain secondary and tertiary structures [75,76]. Alternatively, as the concentration of TFE increases, the solution becomes more homogeneous, reducing the formation of clusters of the cosolvent, which may be associated with the stabilization of α-helices by the excluded volume effect [7,75].

In summary, in this section we show that the simulations are qualitatively consistent with the experimental stabilization of the helix of the $AAQAA_3$ peptide by TFE, both by promoting the helix stability at lower TFE concentrations, and for having a concentration of maximum ellipticity induction.

3.2. Direct interactions and preferential solvation by TFE

In this section, we will analyze the solvation structure of the peptide in solutions of water and TFE. The minimum-distance distribution functions (MDDFs) [53] for water and TFE relative to the peptide are shown in Fig. 3A and 3B, respectively, and depict some similarities: both MDDFs exhibit two well-defined peaks. These peaks follow similar trends as the solutions become more concentrated. The first peaks (at ∼1.8 Å) indicate the presence of specific interactions (hydrogen bonds) with the peptide, while the second peaks (at ∼2.6 Å) are characteristic of the second solvation shell and non-specific interactions. With the increase in TFE concentration, the first peaks of the MDDFs increase, while the second peaks generally decrease. The increase in the first peak is probably associated with the increased hydrophobicity of the solution, which favors direct hydrophilic interactions with the protein. Since the local density augmentation is inversely associated with the potential of mean force, the stability of the hydrogen bonds between water and TFE with the protein is increased when TFE is added to the solution. It is important to note that the increase in the first peak of the water g_{pw} does not mean that the number of hydrogen bonds between the water molecules and the peptide increase, TFE actually substitutes peptide-water hydrogen bonds (data shown in Supplementary Table S1). Yet, the water concentration is very different in the systems containing TFE (Table 2). For example, the concentration in pure water (55.1 mol L^{-1}) is around 4.8 times higher than the concentration of water in the solution with 80 % TFE (11.6 mol L^{-1}, Table 2). Therefore, for the number of hydrogen bonds to be the same in both systems, the peak at ∼1.8 Å in the 80 % TFE solution should have an integral 4.8 times larger. In fact, as the solution becomes more concentrated, TFE molecules are found at shorter distances and compete with the water molecules by hydrogen bonds with the peptide. In parallel, the number of hydrogen bonds between TFE and peptide increases progressively with the addition of TFE to the solution (Table S1).

Despite this stabilization of the water molecules at hydrogen-bonding distances, TFE excludes the water molecules from the second solvation shell and larger distances (from ∼2.0 Å to up to ∼6.5 Å), as shown in Fig. 3A. Non-specific interactions between TFE and the peptide are more pronounced than specific interactions, particularly at smaller TFE concentrations.

Fig. 3C and 3D show the Kirkwood-Buff integrals (KBIs) of water and TFE, respectively. The KBIs determine whether there is excess or exclusion of each solvent component around the solute. In all cases at short distances, r < 1.5 Å, the KBIs display very negative values. This sharp drop reflects the excluded volume of the peptide and the solvent molecules, which can be compensated for by favorable solute–solvent interactions that lead to accumulation in further regions of the solution. The KBI drop of TFE is greater than that of water, because TFE is a bulkier molecule [77].

Only a part of the exclusion volume is compensated by accumulation of water molecules. The KB integrals for water increase after ∼1.5 Å, as shown in Fig. 3C, but are negative at long distances (the qualitative KB trend is consistent, despite their actual convergence not being completely satisfactory in all simulations performed). In Fig. 3D it can be seen that TFE molecules accumulate more effectively on the protein domain than the water molecules and, although the final KB integrals are also negative, they are greater than those of water. For example, in the solution with 20 % of TFE, the TFE KB integrals converge to nearly zero, although this relative density augmentation decreases as the solution becomes more concentrated.

The preferential solvation of the peptide can be quantified by the preferential solvation parameter, Γ_{pc}, calculated from KBIs of the water and the cosolvent (Eq. (6)). The Γ_{pc} values found here are expressed in Table 2. Γ_{pc} is positive for all concentrations. Thus, TFE preferentially solvates the protein, consistently with previous reports [8,9]. This result is interesting because it shows that the accumulation of the cosolvent on the protein surface does not always favor denaturation, as typically observed in, for example, urea or guanidine hydrochloride solutions [78]. On the contrary, we note that TFE preferentially interacts with the peptide and stabilizes the folded helix.

The MDDFs can be decomposed into their atomic contributions and on the contributions of each residue type, providing a detailed molecular interpretation of solute–solvent interactions [51,53]. The decomposition of MDDFs, in essence, reveals the frequency with which each atom (or group of atoms) is closest to any solute atom at each distance, with the sum of all contribution curves equaling the total MDDF. Here, we illustrate the peptide interactions with the solvent using the g_{pc} of the solution at 60 % TFE, but the observed results are qualitatively representative of all concentrations. As shown in Fig. 4A, the specific interactions (H-

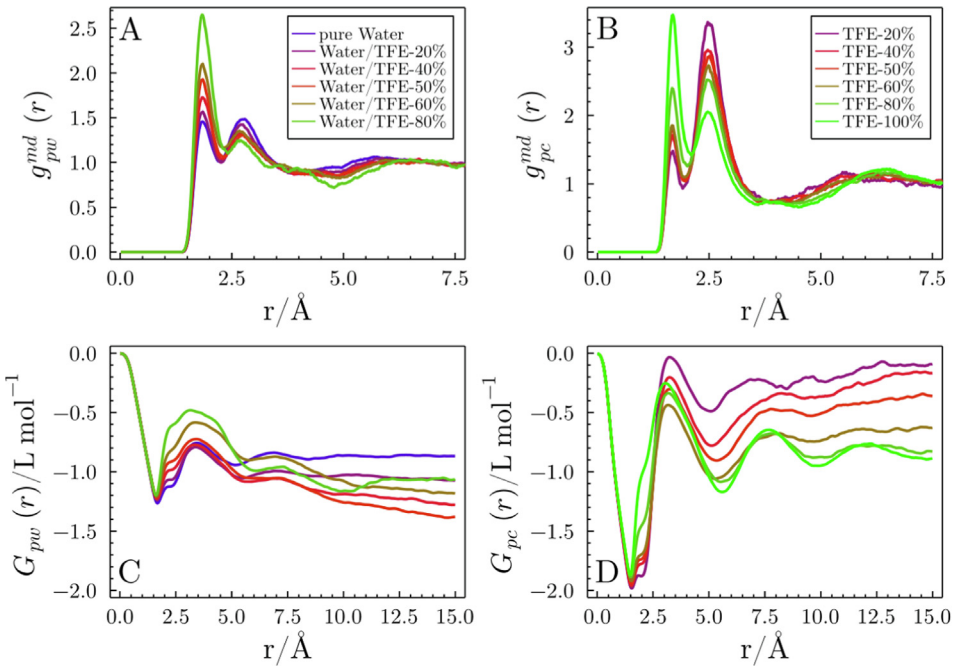

Fig. 3. Minimum-distance distribution functions (MDDFs) A) of water and B) of TFE as a function of the cosolvent concentration. Kirkwood-Buff (KB) integrals for water and TFE are shown in C) and D), respectively.

Table 2
TFE solutions effective concentrations, Kirkwood-Buff integrals for TFE (G_{pc}) and water (G_{pw}) relative to the $(AAQAA)_3$ peptide, and preferential parameter solvation (Γ_{pc}).

Systems	Water concentrations (mol L^{-1})	TFE concentrations (mol L^{-1})	G_{pc} (L × mol^{-1})	G_{pw} (L × mol^{-1})	Γ_{pc}
$AAQAA_3$ – 20 %	45.268	2.757	−0.0862	−1.075	2.727
$AAQAA_3$ – 20 %*	45.381	2.726	1.100	−1.321	6.601
$AAQAA_3$ – 40 %	34.504	5.505	−0.162	−1.280	6.154
$AAQAA_3$ – 40 %*	34.571	5.501	0.00874	−1.462	8.088
$AAQAA_3$ – 50 %	28.933	6.901	−0.366	−1.384	7.023
$AAQAA_3$ – 50 %*	28.880	6.912	−0.562	−1.220	4.549
$AAQAA_3$ – 60 %	23.212	8.294	−0.617	−1.186	4.716
$AAQAA_3$ – 60 %*	23.158	8.311	−0.874	−0.944	0.578
$AAQAA_3$ – 80 %	11.617	11.057	−0.822	−1.060	2.630
$AAQAA_3$ – 80 %*	11.491	11.091	−1.113	0.141	−13.911

* Simulations with modified potentials.

bonds) between the cosolvent and the peptide are completely determined by the contribution of hydroxyl hydrogen (dark gray - H_{TFE}). The H_{TFE} can interact with both the polar residues of the side chain (glutamine residues) (Fig. 4B) and the amide oxygen of the backbone (Fig. 4C). There is no specific interaction between the TFE molecules and the amide nitrogen (Fig. 4C). On the other hand, the non-specific interactions involve predominantly the trifluoro-methyl groups and aliphatic hydrogens of TFE molecules with the nonpolar side chains of the peptide (Fig. 4A and 4B).

The specific interactions between TFE and peptide agree with the direct mechanism proposed by [2] (see Fig. 1) to explain the stabilizing effect of TFE on helices. According to the direct mechanism, TFE molecules interact with the oxygen of the main chain via H-bonds. This interaction, however, can happen without the disruption of the peptide's intramolecular H-bonds ($O_{backbone}$ and $HN_{backbone}$) that would destabilize the helix [2]. At the same time, the trifluoro-methyl group putatively prevents the approach and interaction of water molecules to the amide nitrogen of the main chain. In the next section, we will evaluate the effect of these peptide-TFE H-bonds, and show that they, unexpectedly, favor the unfolded peptide conformations.

3.3. Disrupting the TFE-backbone interaction stabilizes the α-helix

The results presented so far evidently show the helix-stabilizing role of TFE (Fig. 2A and 2B). The interaction modes of the TFE with the peptide, as determined by the characterization of the solvent structure with the MDDFs, support the notion that both direct and indirect mechanisms could be involved in helix stabilization.

In order to probe the role of the direct TFE-backbone interactions in the stabilization of the helix, we have increased the radii associated specifically with the interaction between the polar hydrogen of TFE and the carbonyl oxygens of the peptide backbone. No other interaction was modified. By doing so, we avoid the formation of the H-bonds between these groups, and suppress the possible role of this interaction in the local exclusion of water molecules from the backbone. We expected to demonstrate that water would become a stronger binder to the backbone, competing with the intramolecular hydrogen bonds of the peptide, and thus the helix would be destabilized.

Surprisingly, after modifying the interaction potential to avoid direct interactions between TFE and the backbone, we observe that the α-helix content of the peptide increases significantly. The cir-

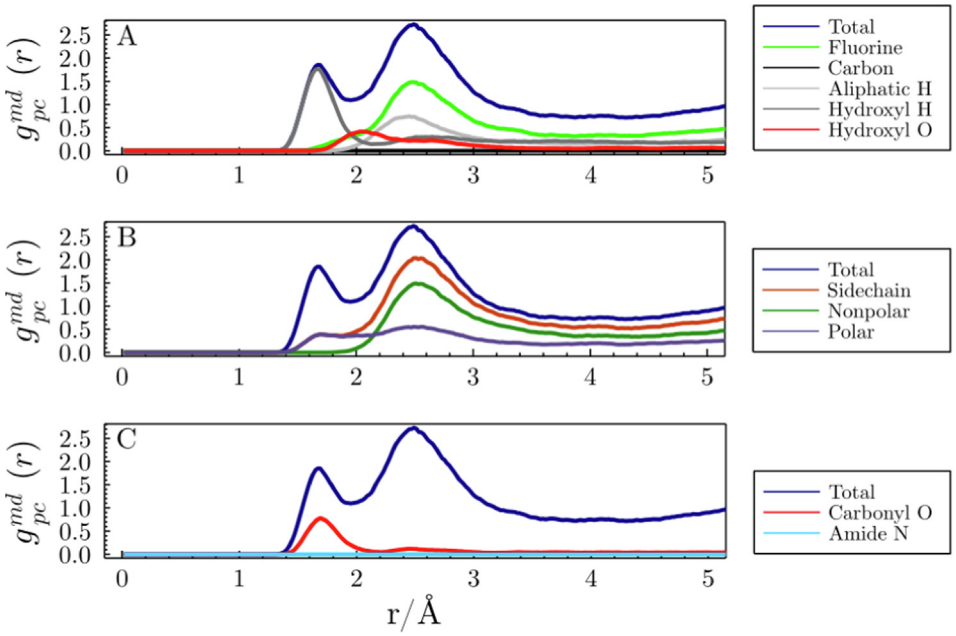

Fig. 4. Minimum-distance distribution function of TFE relative to $AAQAA_3$, and group contributions, in the 60 % vol/vol solution. A) TFE group contribution. B) Peptide sidechain contributions. C) Backbone atom contributions. The only contribution of the backbone atoms to the MDDF of TFE is due to the oxygen atom, which forms H-bonds with the TFE hydroxyl hydrogen.

cular dichroism spectra and the per-residue α-helix content of simulations with modified potentials are shown in Fig. 5A and 5B, for the solution of 80 % vol/vol of TFE in water. The stabilization of the helix was observed in all concentrations, following the disruption of the TFE-backbone hydrogen bond (Figures S3 and S4). It is clear, then, that the direct interactions of TFE with the backbone stabilize unfolded peptide conformations, rather than support the helices.

3.4. Preferential solvation in the absence of the TFE-backbone hydrogen bond

We characterized the solvation structures from the MDDFs to better understand the factors that contribute to the peptide's stabilization and increase in α-helix content in simulations with modified potentials. Once again, we see two distinct peaks in both the water and TFE distribution functions (Fig. 6A and 6B). However, the relative densities of water and TFE molecules in the first and second solvation shells change. At short distances (∼1.8 Å), the relative density of water molecules increases progressively with increasing TFE concentration, as observed with the original potential. On the other hand, the peak associated to TFE molecules remains nearly constant, in sharp contrast with the distributions observed in Fig. 3B for the original interactions. This observation indicates that, with the standard potential, the increase in TFE concentration displaces water molecules from the peptide backbone. This effect is suppressed, and the remaining specific interactions (with the side chain of glutamine residues), occur proportionally to the concentration of TFE.

Because TFE molecules no longer compete with the water for specific interactions with the backbone, the density of water molecules in this region is higher than in the simulations with the standard potentials (Fig. 3A and 6A). Thus, the water affinity to the

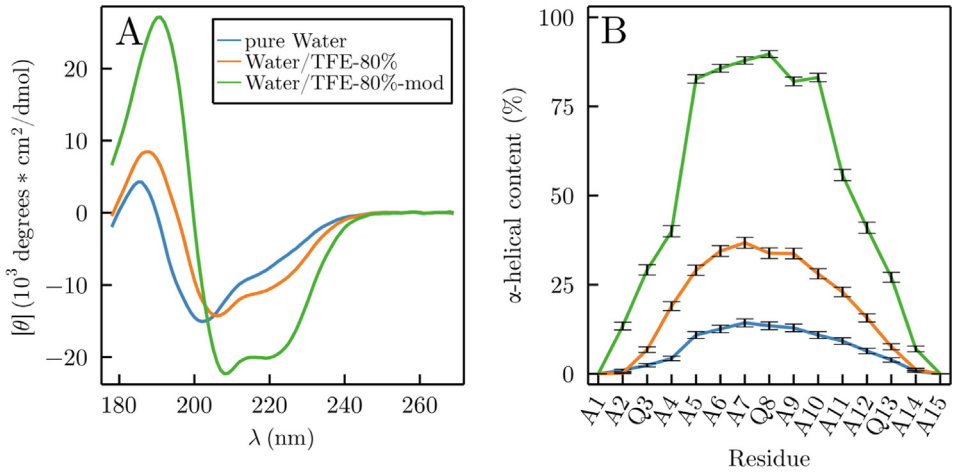

Fig. 5. Structural properties of the $AAQAA_3$ peptide in water (blue) and in 80 % of TFE, computed from the default (orange) simulation and with modified potencial (green): A) Circular dichroism (CD) spectra. B) Average per-reside α-helix prevalence. (For interpretation of the references to colour in this figure legend, the reader is referred to the web version of this article.)

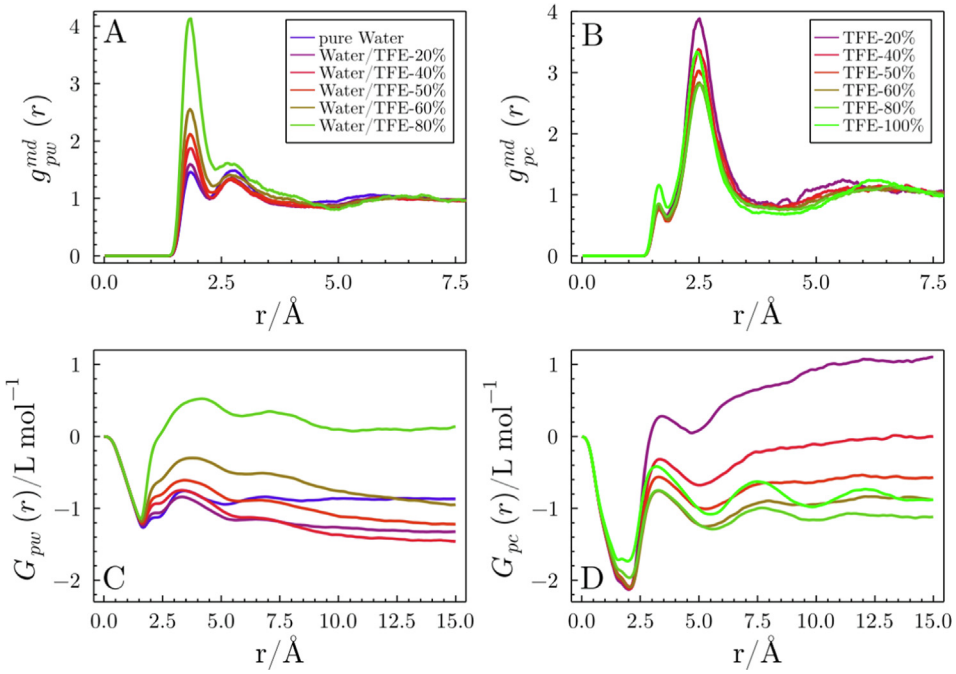

Fig. 6. Minimum-distance distribution functions (MDDFs) A) of water and B) of TFE as a function of the cosolvent concentration for the simulations with modified potentials. Kirkwood-Buff (KB) integrals for water and TFE are shown in C) and D), respectively.

backbone increases, as expected, yet with the unexpected associated result of stabilizing the helix.

Fig. 6C and 6D show the KBIs for water and TFE, respectively, obtained on the modified-potential simulations. The curves' general trend is similar to that of the simulations with the standard potential (Fig. 3C and 3D), but the affinities of the solvent molecules (water and TFE) for the peptide differ. In particular, the KBIs of water and TFE are closer to each other, implying that the preferential solvation by TFE was reduced for most systems, as shown in Table 2. Again, this is expected, as one of the specific interactions of the TFE with the peptide was removed. Nevertheless, for all except the 80 % solution, the preferential solvation parameters are positive and still implies that TFE solvates preferentially the peptide. We note, however, that the peptide structure ensembles are not the same in the simulations with the standard and modified potentials, since the in the later the helical content of the peptide is greater in all simulations, and the peptides display smaller average surface areas (Table S3).

In summary, the simulations with the modified potential led to an increased peptide helical content, in contradiction with the potential stabilizing effect of the TFE-backbone interaction. The peptide remains preferentially solvated by TFE at all but the most concentrated TFE aqueous solution, in the absence of the H-bond with the backbone. Therefore, the non-specific, mostly nonpolar interactions TFE with the peptide are responsible for the preferential solvation and, we conclude (see section 3.5), for the protection of the helical structure. In this sense, our results support those of Roccatano et al. [3], which found that these nonpolar interactions have a role in stabilizing helices. TFE has weak interactions with apolar residues and does not significantly disrupt intra-peptide hydrophobic contacts. In parallel, it has also been reported that the presence of TFE in solution causes a decrease in the local

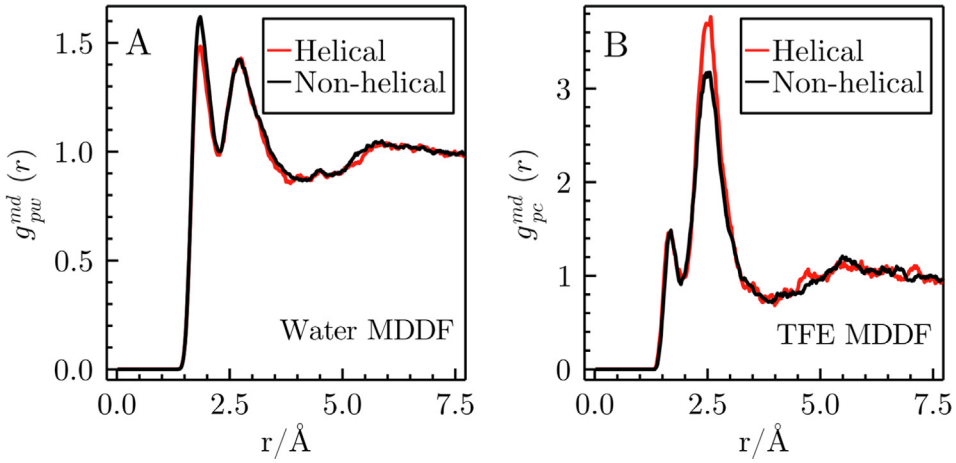

Fig. 7. Minimum-distance distribution functions between the peptide and A) of water and B) TFE in 20 % of TFE for helical (red) and non-helical (black) ensembles. The denatured ensemble forms more hydrogen bonds with water, and displays less non-specific interactions with TFE. (For interpretation of the references to colour in this figure legend, the reader is referred to the web version of this article.)

dielectric constant, which promotes helix formation by strengthening intra-peptide H-bonds, and such effects cannot be disconsidered [15].

3.5. TFE interactions with helical and non-helical ensembles

In the previous sections, we discussed that non-specific interactions with the peptide are responsible for the protective effect of the helices. Here, we cluster the structures of the simulations with the standard potentials into helical and non-helical sets and characterize the solvent structures in each ensemble. Details of the clustering strategy can be found in the Supporting Information (Table S4). Note, from Fig. 2C, that the systems without any helical content represent about ∼60 % of the sampling, while the cluster of structures with ellipticity comprise the other ∼40 % and has about an average of about 40 % of residues in helical conformation. Thus, a significant amount of unstructured peptide is still present in the "helical" ensemble.

Fig. 7A and 7B show the MDDFs of water and of TFE for the helical and non-helical ensembles in the system with 20 % of TFE (the MDDFs for the other systems are shown in Figures S6 (water) and S7 (TFE) and nearly follow the same trend). Fig. 7A shows that the unfolded states, without helical structure, form slightly stronger specific bonds to water than the ensemble of structures with some helical content, supporting the role of water specific interactions in the destabilization of the helices. This can be observed by the increase in the density of water molecules in the first peak of the distribution (∼1.8 Å). Non-specific interactions (second peak) remain roughly constant. Fig. 7B, on the other hand, shows the opposite effect for TFE: the first peak remains constant, but the distribution of TFE molecules decreases in the second peak, indicating that the unfolded states interact less favorably with TFE. As a result of the decrease in the strength of non-specific interactions between peptides and TFE in the non-helical ensemble, water molecules accumulate at short distances. Furthermore, non-specific interactions between TFE and the peptide are stronger in the helical ensemble, corroborating their importance in helix stabilization.

4. Conclusions

We investigated the effects of 2,2,2-Trifluorethanol (TFE) on the conformational equilibrium of the peptide $AAQAA_3$ using enhanced sampling molecular dynamics simulations with the REST2 replica-exchange method to obtain an exhaustive sampling of the folding equilibrium. The ellipticity of the peptide is always greater in the presence of TFE, as shown by computed circular dichroism (CD) spectra and by the direct calculation of the α-helix content. All these findings are consistent with the observed stabilizing effects of TFE [1,8,9,12].

MDDFs demonstrated that TFE interacts with the oxygen of the peptide's backbone via H-bonds and exhibits non-specific interactions with its side chains via the trifluoro-methyl group and aliphatic hydrogens. It competes with the water molecules for specific interactions with the peptide. The peptide is preferentially solvated by TFE at all concentrations. Helical conformations display stronger non-specific interactions with TFE than coil states.

The H-bonds between TFE and the peptide carbonyl backbone is suggestive of a mechanism by which TFE would restrict the access of water molecules to the backbone, preventing it from competing with the intra-helical hydrogen bonds. However, by impairing the interaction potential between the carbonyl oxygen of the backbone and the polar hydrogen of TFE, we investigated the role of this interaction in the stability of the helices. Unexpectedly, the α-helix content increased significantly, implying that the interaction of TFE with the backbone stabilizes the peptide's unfolded state. Even in the absence of this strong polar interaction, the presence of TFE dehydrates the peptide. Therefore, the stabilizing role of TFE on the helix is most likely associated with the "coating" of the helical conformation, which excludes water molecules from the second solvation shell of the backbone and from the first solvation shell of the peptide side chains. Indirect mechanisms associated to the perturbations on the solution structure cannot be ruled out.

CRediT authorship contribution statement

Ander F. Pereira: Conceptualization, Data curation, Validation, Visualization, Formal analysis, Investigation, Methodology, and Writing - original draft, Writing - review & editing. **Vinicius Piccoli:** Conceptualization, Data curation, Validation, Visualization, Formal analysis, Investigation, Methodology, and Writing - original draft, Writing - review & editing. **Leandro Martínez:** Conceptualization, Formal analysis, Funding Acquisition, Validation, Writing - original draft, and Writing - review & editing.

Declaration of Competing Interest

The authors declare that they have no known competing financial interests or personal relationships that could have appeared to influence the work reported in this paper.

Acknowledgements

The authors acknowledge the financial support of Fapesp (2010/16947-9, 2018/24293-0, 2013/08293-7, 2018/14274-9, 2020/04549-0, 2020/04916-3), CNPq (302332/2016-2, 140853/2020-0, 140846/2020-4), and CAPES 206 -04/092018. Research developed with the help of CENAPAD-SP (National Center for High Performance Processing in São Paulo), project UNICAMP / FINEP - MCTI.

References

[1] M. Vincenzi, F.A. Mercurio, M. Leone, About TFE: Old and New Findings, Curr. Protein Pept. Sci. 20 (5) (2019) 425–451.
[2] R. Rajan, P. Balaram, A model for the interaction of trifluoroethanol with peptides and proteins, Int. J. Pep. Protein Res. 48 (2009) 328–336.
[3] D. Roccatano, G. Colombo, M. Fioroni, A.E. Mark, Mechanism by which 2,2,2-trifluoroethanol/water mixtures stabilize secondary-structure formation in peptides: a molecular dynamics study, Proc. Natl. Acad. Sci. USA 99 (19) (2002) 12179–12184.
[4] N. Rezaei-Ghaleh, M. Amininasab, M. Nemat-Gorgani, Conformational changes of alpha-chymotrypsin in a fibrillation-promoting condition: a molecular dynamics study, Biophys. J. 95 (2008) 4139–4147.
[5] M. Buck, Trifluoroethanol and colleagues: cosolvents come of age. Recent studies with peptides and proteins, Q. Rev. Biophys. 31 (1998) 297–355.
[6] D.-P. Hong, M. Hoshino, R. Kuboi, Y. Goto, Clustering of Fluorine-Substituted Alcohols as a Factor Responsible for Their Marked Effects on Proteins and Peptides, J. Am. Chem. Soc. 121 (37) (1999) 8427–8433.
[7] R.M. Culik, R.M. Abaskharon, I.M. Pazos, F. Gai, Experimental validation of the role of trifluoroethanol as a nanocrowder, J. Phys. Chem. B. 118 (39) (2014) 11455–11461.
[8] H. Ohgi, H. Imamura, T. Sumi, K. Nishikawa, Y. Koga, P. Westh, T. Morita, Two different regimes in alcohol-induced coil-helix transition: effects of 2,2,2-trifluoroethanol on proteins being either independent of or enhanced by solvent structural fluctuations, Phys. Chem. Chem. Phys. 23 (2021) 5760–5772.
[9] J. Vymětal, L. Bednárová, J. Vondrášek, Effect of TFE on the Helical Content of AK17 and HAL-1 Peptides: Theoretical Insights into the Mechanism of Helix Stabilization, J. Phys. Chem. B. 120 (2016) 1048–1059.
[10] S. Kumar, K. Modig, B. Halle, Trifluoroethanol-induced beta –> alpha transition in beta-lactoglobulin: hydration and cosolvent binding studied by 2H, 17O, and 19F magnetic relaxation dispersion, Biochemistry. 42 (2003) 13708–13716.
[11] M. Fioroni, M.D. Diaz, K. Burger, S. Berger, Solvation Phenomena of a Tetrapeptide in Water/Trifluoroethanol and Water/Ethanol Mixtures: A Diffusion NMR, Intermolecular NOE, and Molecular Dynamics Study, J. Am. Chem. Soc. 124 (2002) 7737–7744.
[12] A. Kentsis, T.R. Sosnick, Trifluoroethanol promotes helix formation by destabilizing backbone exposure: desolvation rather than native hydrogen

bonding defines the kinetic pathway of dimeric coiled coil folding, Biochemistry. 37 (1998) 14613–14622.
[13] M.D. Díaz, M. Fioroni, K. Burger, S. Berger, Evidence of complete hydrophobic coating of bombesin by trifluoroethanol in aqueous solution: an NMR spectroscopic and molecular dynamics study, Chemistry. 8 (2002) 1663–1669.
[14] R. Walgers, T.C. Lee, A. Cammers-Goodwin, An Indirect Chaotropic Mechanism for the Stabilization of Helix Conformation of Peptides in Aqueous Trifluoroethanol and Hexafluoro-2-propanol, J. Am. Chem. Soc. 120 (20) (1998) 5073–5079.
[15] J.A. Vila, D.R. Ripoll, H.A. Scheraga, Physical reasons for the unusual alpha-helix stabilization afforded by charged or neutral polar residues in alanine-rich peptides, Proc. Natl. Acad. Sci. USA 97 (2000) 13075–13079.
[16] Y.-P. Pang, FF12MC: A revised AMBER forcefield and new protein simulation protocol, Proteins. 84 (2016) 1490–1516.
[17] V. Muñoz, L. Serrano, Elucidating the folding problem of helical peptides using empirical parameters. III. Temperature and pH dependence, J. Mol. Biol. 245 (1995) 297–308.
[18] S.A. Celinski, J.M. Scholtz, Osmolyte effects on helix formation in peptides and the stability of coiled-coils, Protein Sci. 11 (8) (2002) 2048–2051.
[19] E.A. Ploetz, S. Karunaweera, P.E. Smith, Kirkwood-Buff-Derived Force Field for Peptides and Proteins: Applications of KBFF20, J. Chem. Theory Comput. 17 (5) (2021) 2991–3009.
[20] W. Shalongo, L. Dugad, E. Stellwagen, Distribution of helicity within the model peptide acetyl(AAQAA)3amide, J. Am. Chem. Soc. 116 (18) (1994) 8288–8293.
[21] J. Huang, A. MacKerell, Induction of peptide bond dipoles drives cooperative helix formation in the (AAQAA)3 peptide, Biophys. J. 107 (4) (2014) 991–997.
[22] Y. Sugita, Y. Okamoto, Replica-exchange molecular dynamics method for protein folding, Chem. Phys. Lett. 314 (1-2) (1999) 141–151.
[23] K. Hukushima, K. Nemoto, Exchange Monte Carlo method and application to spin glass simulations, J. Phys. Soc. Jpn. 65 (6) (1996) 1604–1608.
[24] K. Hukushima, Extended ensemble Monte Carlo approach to hardly relaxing problems, Comput. Phys. Commun. 147 (1-2) (2002) 77–82.
[25] A. Laio, M. Parrinello, Escaping free-energy minima, Proc. Natl. Acad. Sci. USA 99 (20) (2002) 12562–12566.
[26] C. Tsallis, D.A. Stariolo, Generalized simulated annealing, Physica A. 233 (1-2) (1996) 395–406.
[27] R.H. Swendsen, J.-S. Wang, Replica Monte Carlo simulation of spin glasses, Phys. Rev. Lett. 57 (21) (1986) 2607–2609.
[28] Y.M. Rhee, V.S. Pande, Multiplexed-replica exchange molecular dynamics method for protein folding simulation, Biophys. J. 84 (2) (2003) 775–786.
[29] W. Zheng, M. Andrec, E. Gallicchio, R.M. Levy, Simulating replica exchange simulations of protein folding with a kinetic network model, Proc. Natl. Acad. Sci. USA 104 (39) (2007) 15340–15345.
[30] L. Wang, R.A. Friesner, B.J. Berne, Replica Exchange with Solute Scaling: A More Efficient Version of Replica Exchange with Solute Tempering (REST2), J. Phys. Chem. B 115 (2011) 9431–9438.
[31] P.U. Liu, B. Kim, R.A. Friesner, B.J. Berne, Replica exchange with solute tempering: a method for sampling biological systems in explicit water, Proc. Natl. Acad. Sci. USA 102 (39) (2005) 13749–13754.
[32] X. Huang, M. Hagen, B. Kim, R.A. Friesner, R. Zhou, B.J. Berne, Replica exchange with solute tempering: efficiency in large scale systems, J. Phys. Chem. B. 111 (2007) 5405–5410.
[33] T. Terakawa, T. Kameda, S. Takada, On easy implementation of a variant of the replica exchange with solute tempering in GROMACS, J. Comput. Chem. 32 (7) (2011) 1228–1234.
[34] S.L.C. Moors, S. Michielssens, A. Ceulemans, Improved Replica Exchange Method for Native-State Protein Sampling, J. Chem. Theory Comput. 7 (1) (2011) 231–237.
[35] M.J. Abraham, T. Murtola, R. Schulz, S. Páll, J.C. Smith, B. Hess, E. Lindahl, GROMACS: High performance molecular simulations through multi-level parallelism from laptops to supercomputers, SoftwareX. 1–2 (2015) 19–25.
[36] M. Bonomi, D. Branduardi, G. Bussi, C. Camilloni, D. Provasi, P. Raiteri, D. Donadio, F. Marinelli, F. Pietrucci, R.A. Broglia, M. Parrinello, PLUMED: A portable plugin for free-energy calculations with molecular dynamics, Comput. Phys. Commun. 180 (2009) 1961–1972.
[37] M. Parrinello, A. Rahman, Polymorphic transitions in single crystals: A new molecular dynamics method, J. Appl. Phys. 52 (1981) 7182–7190.
[38] G. Bussi, D. Donadio, M. Parrinello, Canonical sampling through velocity rescaling, J. Chem. Phys. 126 (2007) 014101.
[39] T. Darden, D. York, L. Pedersen, Particle mesh Ewald: AnN·log(N) method for Ewald sums in large systems, J. Chem. Phys. 98 (1993) 10089–10092.
[40] B. Hess, H. Bekker, H.J.C. Berendsen, J.G.E. Fraaije, LINCS: A linear constraint solver for molecular simulations, J. Comput. Chem. 18 (1997) 1463–1472.
[41] W. Humphrey, A. Dalke, K. Schulten, VMD: Visual molecular dynamics, J. Mol. Graphics. 14 (1996) 33–38.
[42] J.M. Martínez, L. Martínez, Packing optimization for automated generation of complex system's initial configurations for molecular dynamics and docking, J. Comput. Chem. 24 (2003) 819–825.
[43] L. Martínez, R. Andrade, E.G. Birgin, J.M. Martínez, PACKMOL: a package for building initial configurations for molecular dynamics simulations, J. Comput. Chem. 30 (2009) 2157–2164.
[44] J.L.F. Abascal, C. Vega, A general purpose model for the condensed phases of water: TIP4P/2005, J. Chem. Phys. 123 (23) (2005) 234505.
[45] R.B. Best, J. Mittal, Protein simulations with an optimized water model: cooperative helix formation and temperature-induced unfolded state collapse, J. Phys. Chem. B. 114 (2010) 14916–14923.
[46] J. Vymětal, J. Vondrášek, Parametrization of 2,2,2-trifluoroethanol based on the generalized AMBER force field provides realistic agreement between experimental and calculated properties of pure liquid as well as water-mixed solutions, J. Phys. Chem. B. 118 (35) (2014) 10390–10404.
[47] P. Robustelli, S. Piana, D.E. Shaw, Developing a molecular dynamics force field for both folded and disordered protein states, Proc. Natl. Acad. Sci. U. S. A. 115 (2018) E4758–E4766.
[48] W. Kabsch, C. Sander, Dictionary of protein secondary structure: pattern recognition of hydrogen-bonded and geometrical features, Biopolymers. 22 (1983) 2577–2637.
[49] G. Nagy, M. Igaev, N.C. Jones, S.V. Hoffmann, H. Grubmüller, SESCA: Predicting Circular Dichroism Spectra from Protein Molecular Structures, J. Chem. Theory Comput. 15 (2019) 5087–5102.
[50] G. Nagy, C. Oostenbrink, Dihedral-based segment identification and classification of biopolymers I: proteins, J. Chem. Inf. Model. 54 (1) (2014) 266–277.
[51] L. Martínez, ComplexMixtures.jl: Investigating the structure of solutions of complex-shaped molecules from a solvent-shell perspective, J. Mol. Liq. 347 (2022) 117945.
[52] V. Piccoli, L. Martínez, Correlated counterion effects on the solvation of proteins by ionic liquids, J. Mol. Liq. 320 (2020) 114347.
[53] L. Martínez, S. Shimizu, Molecular Interpretation of Preferential Interactions in Protein Solvation: A Solvent-Shell Perspective by Means of Minimum-Distance Distribution Functions, J. Chem. Theory Comput. 13 (2017) 6358–6372.
[54] I.P. de Oliveira, L. Martínez, The shift in urea orientation at protein surfaces at low pH is compatible with a direct mechanism of protein denaturation, Phys. Chem. Chem. Phys. 22 (1) (2020) 354–367.
[55] S. Shimizu, C.L. Boon, The Kirkwood-Buff theory and the effect of cosolvents on biochemical reactions, J. Chem. Phys. 121 (18) (2004) 9147–9155.
[56] S. Shimizu, N. Matubayasi, Preferential hydration of proteins: A Kirkwood-Buff approach, Chemical Physics Letters. 420 (4-6) (2006) 518–522.
[57] D. Harries, J. Rösgen, A practical guide on how osmolytes modulate macromolecular properties, Methods Cell Biol. 84 (2008) 679–735.
[58] E.A. Oprzeska-Zingrebe, J. Smiatek, Aqueous ionic liquids in comparison with standard co-solutes : Differences and common principles in their interaction with protein and DNA structures, Biophys. Rev. 10 (2018) 809–824.
[59] M.A. Schroer, J. Michalowsky, B. Fischer, J. Smiatek, G. Grübel, Stabilizing effect of TMAO on globular PNIPAM states: preferential attraction induces preferential hydration, Phys. Chem. Chem. Phys. 18 (2016) 31459–31470.
[60] P.E. Smith, Equilibrium dialysis data and the relationships between preferential interaction parameters for biological systems in terms of Kirkwood-Buff integrals, J. Phys. Chem. B. 110 (6) (2006) 2862–2868.
[61] E.S. Courtenay, M.W. Capp, C.F. Anderson, M.T. Record Jr, Vapor pressure osmometry studies of osmolyte-protein interactions: implications for the action of osmoprotectants in vivo and for the interpretation of "osmotic stress" experiments in vitro, Biochemistry. 39 (2000) 4455–4471.
[62] M.T. Record, C.F. Anderson, Interpretation of preferential interaction coefficients of nonelectrolytes and of electrolyte ions in terms of a two-domain model, Biophys. J. 68 (3) (1995) 786–794.
[63] D.R. Canchi, A.E. García, Cosolvent effects on protein stability, Annu. Rev. Phys. Chem. 64 (1) (2013) 273–293.
[64] I.L. Shulgin, E. Ruckenstein, A protein molecule in an aqueous mixed solvent: fluctuation theory outlook, J. Chem. Phys. 123 (2005) 054909.
[65] I.L. Shulgin, E. Ruckenstein, A protein molecule in a mixed solvent: the preferential binding parameter via the Kirkwood-Buff theory, Biophys. J. 90 (2006) 704–707.
[66] B.M. Baynes, B.L. Trout, Proteins in Mixed Solvents: A Molecular-Level Perspective, J. Phys. Chem. B. 107 (2003) 14058–14067.
[67] A. Jasanoff, A.R. Fersht, Quantitative determination of helical propensities from trifluoroethanol titration curves, Biochemistry. 33 (8) (1994) 2129–2135.
[68] P. Luo, R.L. Baldwin, Mechanism of helix induction by trifluoroethanol: a framework for extrapolating the helix-forming properties of peptides from trifluoroethanol/water mixtures back to water, Biochemistry. 36 (1997) 8413–8421.
[69] A. Chakrabartty, T. Kortemme, S. Padmanabhan, R.L. Baldwin, Aromatic side-chain contribution to far-ultraviolet circular dichroism of helical peptides and its effect on measurement of helix propensities, Biochemistry. 32 (21) (1993) 5560–5565.
[70] Y. Fezoui, D.B. Teplow, Kinetic studies of amyloid beta-protein fibril assembly. Differential effects of alpha-helix stabilization, J. Biol. Chem. 277 (2002) 36948–36954.
[71] D. Hamada, Y. Kuroda, T. Tanaka, Y. Goto, High helical propensity of the peptide fragments derived from beta-lactoglobulin, a predominantly beta-sheet protein, J. Mol. Biol. 254 (1995) 737–746.
[72] M. Ndao, K. Dutta, K.M. Bromley, R. Lakshminarayanan, Z. Sun, G. Rewari, J. Moradian-Oldak, J.S. Evans, Probing the self-association, intermolecular contacts, and folding propensity of amelogenin, Protein Sci. 20 (4) (2011) 724–734.
[73] C.M. Othon, O.-H. Kwon, M.M. Lin, A.H. Zewail, Solvation in protein (un)folding of melittin tetramer-monomer transition, Proc. Natl. Acad. Sci. USA 106 (31) (2009) 12593–12598.
[74] C.A. Rohl, A. Chakrabartty, R.L. Baldwin, Helix propagation and N-cap propensities of the amino acids measured in alanine-based peptides in 40 volume percent trifluoroethanol, Protein Sci. 5 (12) (1996) 2623–2637.
[75] B. Chaubey, A. Dey, A. Banerjee, N. Chandrakumar, S. Pal, Assessment of the Role of 2,2,2-Trifluoroethanol Solvent Dynamics in Inducing Conformational

Transitions in Melittin: An Approach with Solvent F Low-Field NMR Relaxation and Overhauser Dynamic Nuclear Polarization Studies, J. Phys. Chem. B. 124 (2020) 5993–6003.
[76] A. Cammers-Goodwin, T.J. Allen, S.L. Oslick, K.F. McClure, J.H. Lee, D.S. Kemp, Mechanism of stabilization of helical conformations of polypeptides by water containing trifluoroethanol, J. Am. Chem. Soc. 118 (13) (1996) 3082–3090.
[77] A.R. Van Buuren, H.J. Berendsen, Molecular dynamics simulation of the stability of a 22-residue alpha-helix in water and 30% trifluoroethanol, Biopolymers. 33 (1993) 1159–1166.
[78] W. Zheng, A. Borgia, K. Buholzer, A. Grishaev, B. Schuler, R.B. Best, Probing the Action of Chemical Denaturant on an Intrinsically Disordered Protein by Simulation and Experiment, J. Am. Chem. Soc. 138 (36) (2016) 11702–11713.